Structure and Mechanism of MbtI, the Salicylate Synthase from *Mycobacterium tuberculosis*†

Jacque Zwahlen,[‡,§] Subramaniapillai Kolappan,[§,||,⊥] Rong Zhou,[‡] Caroline Kisker,*[,||,#] and Peter J. Tonge*[,‡]

Department of Chemistry, Stony Brook University, Stony Brook, New York 11794-3400, Department of Pharmacological Sciences and Center for Structural Biology, Stony Brook University, Stony Brook, New York 11794-5115, and Rudolf Virchow Center for Experimental Biomedicine, Institute for Structural Biology, University of Würzburg, Versbacher Str. 9, 97078 Würzburg, Germany

Received May 1, 2006; Revised Manuscript Received August 29, 2006

ABSTRACT: MbtI (*rv2386c*) from *Mycobacterium tuberculosis* catalyzes the initial transformation in mycobactin biosynthesis by converting chorismate to salicylate. We report here the structure of MbtI at 2.5 Å resolution and demonstrate that isochorismate is a kinetically competent intermediate in the synthesis of salicylate from chorismate. At pH values below 7.5 isochorismate is the dominant product while above this pH value the enzyme converts chorismate to salicylate without the accumulation of isochorismate in solution. The salicylate and isochorismate synthase activities of MbtI are Mg^{2+}-dependent, and in the absence of Mg^{2+} MbtI has a promiscuous chorismate mutase activity similar to that of the isochorismate pyruvate lyase, PchB, from *Pseudomonas aeruginosa*. MbtI is part of a larger family of chorismate-binding enzymes descended from a common ancestor (the MST family), that includes the isochorismate synthases and anthranilate synthases. The lack of active site residues unique to pyruvate eliminating members of this family, combined with the observed chorismate mutase activity, suggests that MbtI may exploit a sigmatropic pyruvate elimination mechanism similar to that proposed for PchB. Using a combination of structural, kinetic, and sequence based studies we propose a mechanism for MbtI applicable to all members of the MST enzyme family.

The biosynthesis of mycobactin, an essential siderophore and virulence factor in *Mycobacterium tuberculosis*, is initiated by the conversion of chorismate to salicylate catalyzed by MbtI[1] (*rv2386c*) (Figure 1) (*1*−*4*). MbtI is a member of a larger family of chorismate binding enzymes descended from a common ancestor. This Mg^{2+} dependent family (*5*) catalyzes the initial transformations in menaquinone (*6*−*8*), siderophore (*4*, *9*), and tryptophan (*10*−*12*) biosynthesis and will be referred to as the MST family. Based on studies with MenF, the menaquinone-specific isochorismate synthase from *Escherichia coli*, we have recently proposed a model for isomerization in this enzyme family (*8*). In the present work we extend the studies on MenF to MbtI, and propose that MbtI, as well as anthranilate synthase (AS, Figure 1), catalyzes pyruvate elimination via a concerted sigmatropic mechanism similar to that established for isochorismate pyruvate lyase, PchB, from *Pseudomonas aeruginosa* (*13*−*15*).

Chorismate and isochorismate are highly functionalized molecules that, in addition to numerous enzymatic reactions, undergo at least two spontaneous transformations (*13*−*15*). These include the sigmatropic rearrangements leading to the corresponding prephenate and hydroxybenzoate molecules (Figure 2). Isotopic labeling studies by Hilvert and coworkers (*13*−*15*) have established that the spontaneous fates of chorismate and isochorismate are controlled by the orientation of their pyruvate side chains. Relevant for MbtI, this dependence on side chain orientation has been extended to the elimination of pyruvate from isochorismate catalyzed by PchB (*13*, *15*). Various *Pseudomonas* species use a pyochelin siderophore for the establishment and maintenance of infection (*4*). Like both mycobactin and the *Yersinia* siderophore yersiniabactin, pyochelin is derived from salicylate. Unlike *M. tuberculosis* and *Yersinia*, pseudomonads use the combined activity of isochorismate synthase, PchA,

† This work was supported by National Institutes of Health Research Grant AI58785 (to P.J.T.). J.Z. was partially supported by a GAANN (Graduate Assistance In Areas Of National Need) Fellowship.

* To whom correspondence should be addressed. P.J.T.: Department of Chemistry, Stony Brook University, Stony Brook, NY 11794-3400; tel, (631) 632 7907; fax, (631) 632 7934; e-mail, peter.tonge@sunysb.edu. C.K.: Rudolf Virchow Center for Experimental Biomedicine, Institute for Structural Biology, University of Würzburg, Versbacher Str. 9, 97078 Würzburg, Germany; tel, +0931 201 48300; fax, +0931 201 48309; e-mail, caroline.kisker@virchow.uni-wuerzburg.de.

‡ Department of Chemistry.

§ These authors contributed equally to the work.

|| Department of Pharmacological Sciences and Center for Structural Biology.

⊥ Present address: Simon Fraser University, Department of Molecular Biology and Biochemistry, Burnaby, BC Canada, V5A 1S6.

Rudolf Virchow Center for Experimental Biomedicine.

[1] Abbreviations: MbtI, the salicylate synthase from *Mycobacterium tuberculosis*; PchB, isochorismate pyruvate lyase; Irp9, the salicylate synthase from *Yersinia enterocolitica*; YbtS the salicylate synthase from *Yersinia pestis*; MenF, the menaquinone specific isochorismate synthase; PabB, aminodeoxychorismate synthase; AS, anthranilate synthase; MST, the related enzymes catalyzing the initial transformations in menaquinone, siderophore, and tryptophan biosynthesis; AS-sm, the anthranilate synthase from *Serratia marcescens*; AS-ss, the anthranilate synthase from *Sulfolobus solfataricus*; AS-st, the anthranilate synthase from *Salmonella typhimurium*; ICS, isochorismate synthase; BsCM, the chorismate mutase from *Bacillus subtilis*.

10.1021/bi060852x CCC: $37.00
Published on Web 01/06/2007

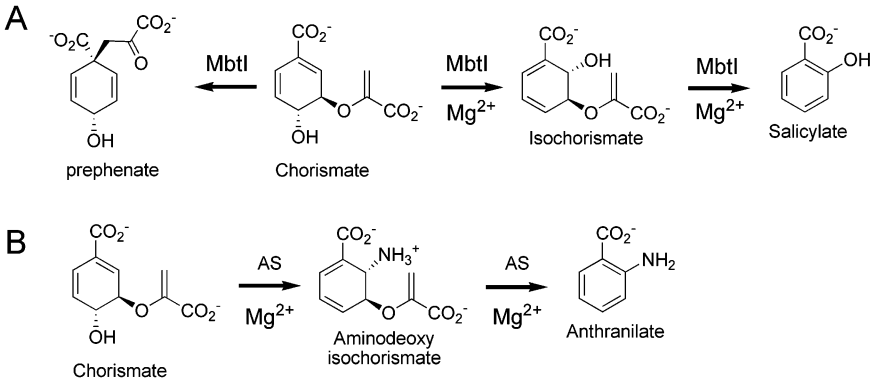

FIGURE 1: Reactions catalyzed by MbtI and AS. (A) Four activities can be detected for wild-type MbtI. In the presence of Mg^{2+} the enzyme catalyzes the formation of isochorismate and salicylate from chorismate, and will also accept isochorismate directly as a substrate. In the absence of Mg^{2+}, the enzyme catalyzes the formation of prephenate from chorismate. (B) Anthranilate synthase (AS) catalyzes the formation of anthranilate from chorismate via aminodeoxyisochorismate.

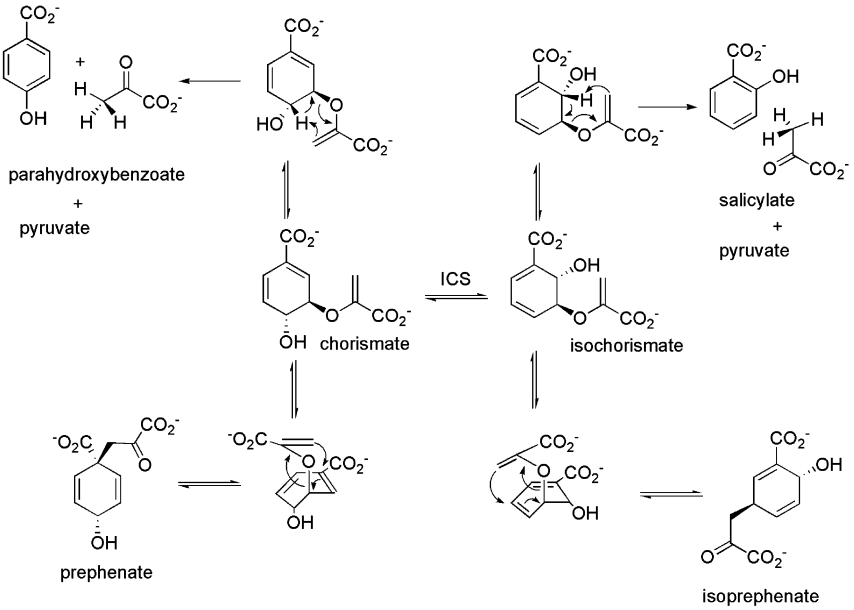

FIGURE 2: Nonenzymatic sigmatropic rearrangements of chorismate and isochorismate. Chorismate and isochorismate are highly flexible metabolites that undergo nonenzymatic sigmatropic rearrangements to prephenate/isoprephenate and parahydroxybenzoate/salicylate, respectively.

and isochorismate pyruvate lyase, PchB, for salicylate biosynthesis (Figure 3) (*16*, *17*). MbtI and PchB both catalyze the elimination of pyruvate from isochorismate and, as shown in the present work for MbtI, also have promiscuous chorismate mutase activities (*16*) suggesting mechanistic commonalities despite the lack of sequence homology. Surprisingly neither enzyme contains the obvious active site machinery to facilitate pyruvate elimination (*15*).

The crystal structure of the MbtI homologue AS from *Serratia marcescens* (AS-sm) has been reported in complex with benzoate, pyruvate, and Mg^{2+} (*12*). This structure, combined with biochemical data (*18*, *19*), supported a base-assisted mechanism for pyruvate elimination in the MST family (*20*) (Figure 4). Saturation mutagenesis of AS-sm His398 identified a Met substitution that resulted in an accumulation of the aminodeoxychorismate (ADIC) intermediate (*18*). As this residue is 3.8 Å from the aromatic product in the AS-sm structure, it was concluded that His398 is the base that abstracts the C2 ADIC proton leading to pyruvate elimination (*12*). However, recent structural (*21*) and modeling (*22*) studies have established that His398 is incorrectly positioned to abstract the C2 proton and is in fact located on the opposite side of the substrate molecule. In addition, His398 is almost universally conserved throughout the MST family and is present in enzymes such as MenF, which do not catalyze pyruvate elimination. We report here the crystal structure of MbtI and, based on comparative biochemical and structural studies, present a new model for pyruvate elimination in the MST enzyme family.

MATERIALS AND METHODS

Preparation of Substrates. Chorismate was purified from *E. coli* KA12 cells as previously described (*23*). Isochorismate was prepared by incubation of chorismate with *E. coli* MenF in a reaction mixture containing 50 mM Tris-HCl pH 7−8, chorismate, and 1 mM Mg^{2+} followed by HPLC purification using a Waters X-terra C-18 semiprep column (*7*). Chromatography was performed using 5% acetic acid in H_2O for 16 min at a flow rate of 1.3 mL/min, after which the concentration of acetonitrile was linearly increased to 100% at 23 min. Isochorismate and chorismate had retention times of 9 and 11 min, respectively. Reaction mixtures were

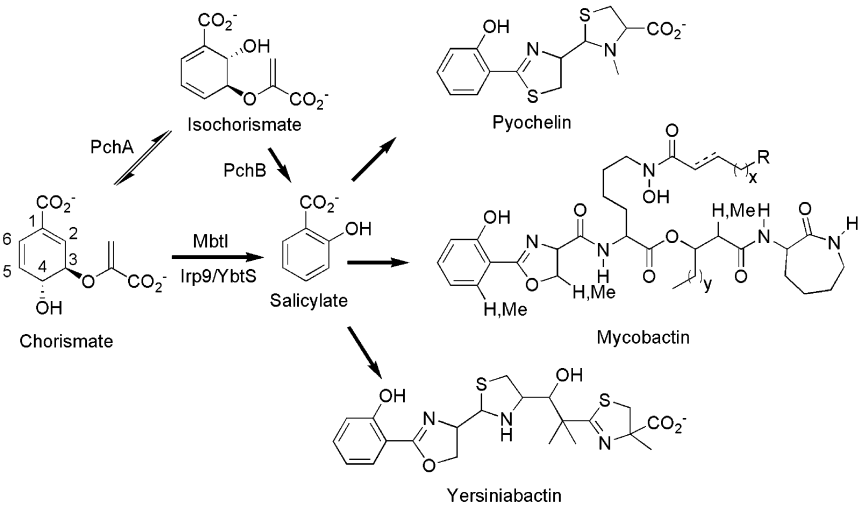

FIGURE 3: The salicylate-derived siderophores pyochelin, mycobactin, and yersiniabactin. These non-ribosomal peptide/polyketide molecules are virulence factors whose biosynthesis begins with the conversion of chorismate to salicylate. In *Yersinia* and *M. tuberculosis* this is achieved by the activity of a single enzyme, Irp9/YbtS and MbtI, respectively. In *Pseudomonas* species, salicylate is formed by the concerted activity of PchA and PchB. Chorismate numbering is shown.

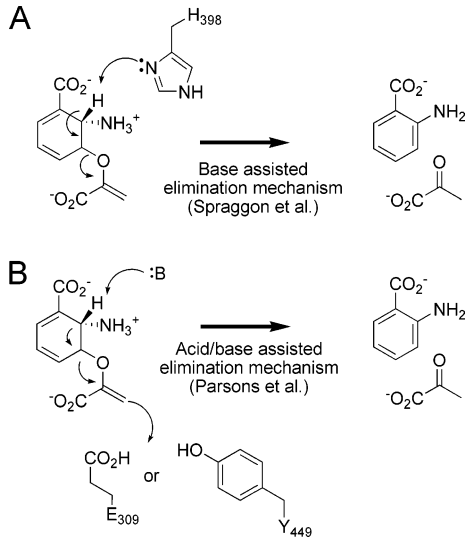

FIGURE 4: Previous mechanisms proposed for pyruvate elimination in the MST family. (A) Mutagenesis and structural studies of AS-sm were originally interpreted to support a base assisted elimination mechanism in which abstraction of the C2 proton by a conserved His leads to elimination of pyruvate (*12*). (B) An acid/base assisted mechanism in which an unidentified base abstracts the C2 proton with protonation of the enolpyruvyl group by either a conserved Glu or Tyr was proposed by Parsons et al. (*35*). Residue numbering is based on AS-sm.

monitored using absorption spectroscopy, and 100 μL aliquots were combined with 400 μL of 5% acetic acid prior to injection.

Protein Expression and Purification. The MbtI gene was amplified from $H37_{Rv}$ genomic DNA using the primers 5′-GGAATTCCATATGTCCGAGCTCAGCGTCGC-3′ (forward) and 5′-CCGCTCGAGTTACTGGCGTGCAACCAGATAAGGCG-3′ (reverse), and cloned into Novagen's pET-15b vector using the *Nde*I and *Xho*I restriction sites (underlined). MbtI was expressed in BL21(DE3) cells as previously described for *E. coli* MenF (*7*) and purified using Novagen His-bind metal affinity resin according to the manufacturer's instructions. After metal affinity chromatography, MbtI was exchanged into 50 mM Tris-HCl, 0.1 mM EDTA pH 7.5 using a Sephadex G-25 column and concentrated to 25 mg/mL using a Millipore YM-30 centriplus. Protein purified using this procedure was shown to be greater than 95% homogeneous using SDS−PAGE, and was stored in 60 μL aliquots at −80 °C after flash freezing in liquid N_2. Selenomethionine (Se-Met) labeled MbtI was prepared as described for *E. coli* MenF (*8*). Attempts to assess whether the N-terminal His-tag affected activity were hindered by our inability to completely remove the tag using thrombin. Consequently, the MbtI gene was recloned into an intein-chitin based vector pTXB1 (New England Biolabs) resulting in a tag free protein after cleavage with DTT on the chitin column. Tag free MbtI was found to have identical kinetic properties to the His-tagged variant. Since the His-tagged protein was purified in 10-fold greater yields than the intein-based method, His-tagged MbtI was used for all remaining studies. The His-tag purification method was also used for the Lys205Ala, Glu252Gln, Leu268Ala, Thr271Ala, His334Met, and Arg405Ala MbtI mutants which were constructed using QuickChange mutagenesis (Stratagene, La Jolla, CA).

While metal affinity chromatography provided wild-type (WT) and mutant proteins that were greater than 95% pure based on SDS−PAGE, an additional purification step was introduced in an attempt to ascertain whether the chorismate mutase activity, observed for WT MbtI in the absence of Mg^{2+} and in some of the mutant MbtI proteins (see below), was the result of a contaminating enzyme that copurified with MbtI. Consequently, concentrated enzyme samples obtained following His-tag purification were applied to a 1.5 × 7.5 cm Q-sepharose column equilibrated with 100 mL of 50 mM Tris-HCl pH 7.5 (buffer A). After washing with 100 mL of buffer A, MbtI was eluted with a linear gradient of 0−0.4 M NaCl in buffer A. Fractions containing MbtI, which eluted at a salt concentration of around 0.2 M, were combined, concentrated, and dialyzed against 2 L of 50 mM Tris-HCl pH 7.5 containing 0.1 mM EDTA for storage.

Enzyme Activity. Isochorismate pyruvate lyase and salicylate synthase activities were measured at pH 8.0 by coupling the elimination of pyruvate to lactate dehydrogenase. Isochorismate synthase activity was measured at pH

7.0 using lactate dehydrogenase to monitor the formation of pyruvate following the action of EntB on isochorismate. EntB is the *E. coli* isochorismatase enzyme that converts isochorismate into pyruvate and 2,3-dihydro-2,3,-dihydroxybenzoate as part of enterobactin biosynthesis (*24*, *25*). Chorismate mutase activity was measured at pH 7.5 by monitoring the formation of phenylpyruvate generated upon acid hydrolysis of prephenate (*16*). Reactions were also monitored using UV−visible absorption spectroscopy to follow the time-dependent changes in the concentration of chorismate, (λ_{max} 274 nm, ϵ 2630 M^{-1} cm^{-1}), isochorismate (λ_{max} 278 nm, ϵ 8300 M^{-1} cm^{-1}) and salicylate (λ_{max} 295 nm, ϵ 2968 M^{-1} cm^{-1}). All reactions were performed in 100 mM Tris-HCl buffer at 37 °C using a Varian CARY 100 spectrophotometer. Steady-state kinetic parameters were determined by varying the concentration of chorismate or isochorismate from 0 to 1 mM. For the Mg^{2+}-dependent reactions, the concentration of Mg^{2+} was maintained at 1 mM, it having been first demonstrated that this concentration of Mg^{2+} was saturating. In addition to absorption spectroscopy, the conversion of chorismate into isochorismate and salicylate was routinely monitored by HPLC, as described above for the purification of isochorismate, under which conditions salicylate had a retention time of 23 min.

Crystallization. WT MbtI (25 mg/mL) was crystallized by vapor diffusion. 1 μL of MbtI was mixed with 1 μL of a reservoir solution containing 0.1 M sodium acetate pH 4.6 and 2 M sodium formate and equilibrated against the same reservoir solution. Se-Met MbtI (25 mg/mL) crystals were grown under identical conditions using WT MbtI crystals for microseeding.

Data Collection and Structure Determination. Diffraction data were collected at beamline X26C at the National Synchrotron Light Source, Brookhaven National Laboratory. For Se-Met labeled crystals, the wavelengths were chosen on the basis of the fluorescence spectrum taken at the beamline. Data were collected for two wavelengths corresponding to a high energy remote wavelength (0.9745 Å) and the inflection point (0.97971 Å). WT and Se-Met MbtI crystals diffracted to 2.5 Å and 3.1 Å, respectively. All data sets were processed, scaled, and integrated using HKL2000 (*26*). Both WT and Se-Met crystals belong to the orthorhombic space group $C222_1$ with $a = 49.2$ Å, $b = 143.6$ Å, and $c = 123.8$ Å and contain one molecule in the asymmetric unit. Se-MET data were used for the initial phase determination using SOLVE (*27*). SOLVE located all six selenium positions, which were used for initial phasing. The phases were further improved by density modification using RESOLVE (*28*), and a clear interpretable electron density map was obtained, which was extended to the full resolution using DM (*29*). The model was built manually with O (*30*). After a few cycles of model building and restrained refinement (*31*), the R_{free} was 0.301 for the resolution range of 25 to 2.5 Å. At this stage water molecules were added, and after a few cycles of further refinement the stereochemistry of the model was checked with PROCHECK (*32*). Data and refinement statistics are shown in Table 1.

NMR Spectroscopy. ^{1}H NMR experiments were performed on a Varian INOVA 500 MHz spectrometer at 30 °C using the PRESAT gradient spin echo sequence for solvent suppression. NMR samples (0.7 mL) were prepared in 20 mM potassium phosphate D_2O buffer pD 7.8 containing 5 mM $MgCl_2$. A series of NMR spectra were collected every 15 min over a 240 min period following the addition of 25 μM MbtI to a sample containing 2 mM chorismate.

Table 1: Data Collection and Refinement Statistics[a]

	Se-inflection	Se-remote	native
Data Collection			
space group	$C222_1$	$C222_1$	$C222_1$
wavelength (Å)	0.9797	0.9745	0.97971
resolution (Å)	3.2	3.2	2.5
no. of reflections (measd)	54487	54729	61810
no. of reflections (unique)	7746	7747	15648
completeness (%)	99.9 (100)	99.9(99.9)	99.1 (98.2)
R_{merge} (%)	6.3 (33.2)	5.7 (32.1)	6.2 (77.1)
$\langle I\rangle/\langle\sigma I\rangle$	25.4 (5.3)	25.9 (5.6)	21.4 (2.0)
no. of sites	6		
mean figure of merit 3.2 Å	0.52		
Refinement			
resolution range (Å)			25−2.5
reflections			14693
R_{cryst}			0.235
R_{free}			0.294
no. of atoms			
protein			3088
water			3
deviations from ideal values			
in bond lengths (Å)			0.014
in angles (deg)			1.822
average *B* factor (Å^2)			52.0
Ramachandran statistics (%)			85.2/10.9/2.2/1.7

[a] $R_{merge} = \sum_{hkl}\sum_i|I_i - \langle I\rangle|/\sum_{hkl}\sum_i$I where I_i is the *i*th measurement and $\langle I\rangle$ is the weighted mean of all measurements of *I*. $\langle I\rangle/\langle\sigma I\rangle$ indicates the average of the intensity divided by its average standard deviation. Numbers in parentheses refer to the respective highest resolution data shell in each data set. $R_{cryst} = \sum||F_o| - |F_c||/\sum|F_o|$ where F_o and F_c are the observed and calculated structure factor amplitudes. R_{free} same as R_{cryst} for 5% of the data randomly omitted from the refinement. Ramachandran statistics indicate the fraction of residues in the most favored, additionally allowed, generously allowed, and disallowed regions of the Ramachandran diagram, as defined by the program PROCHECK (*32*).

Table 2: Kinetic Evaluation of Wild-Type (WT) MbtI Activities in the Presence of Mg^{2+}

activity[a]	k_{cat} (min^{-1})	K_m (μM)	k_{cat}/K_m (μM^{-1} min^{-1})
isochorismate synthase	3.1 ± 0.4	34 ± 11	0.09 ± 0.04
isochorismate pyruvate lyase	2.1 ± 0.1	2.6 ± 0.3	0.81 ± 0.13
salicylate synthase	2.8 ± 0.2	6 ± 5	0.5 ± 0.4

[a] Isochorismate synthase activity was measured at pH 7 while the isochorismate pyruvate lyase and salicylate synthase activities were determined at pH 8. For the isochorismate pyruvate lyase activity, isochorismate was used as the substrate. Reactions were performed in 100 mM Tris-HCl buffer at 37 °C as described in the text.

RESULTS

Enzyme Kinetics. Four distinct activities can be detected for MbtI in vitro (Figure 1). These include isochorismate synthase, isochorismate pyruvate lyase, salicylate synthase (Table 2), and chorismate mutase (Table 3). The first three activities require the presence of Mg^{2+} while chorismate mutase activity is observed for WT MbtI in the absence of Mg^{2+}. For MbtI, the formation of isochorismate can be detected by coupling the reaction to the isochorismatase, EntB (*24*, *25*). Accumulation of isochorismate at pH values below 7.5 can be observed using UV−vis absorption spectroscopy and HPLC analysis of reaction mixtures. At

Table 3: Chorismate Mutase Activity of Wild-Type (WT) and Mutant MbtIs

enzyme[a]	k_{cat} (min^{-1})	K_m (μM)	k_{cat}/K_m (μM^{-1} min^{-1})
wild-type	4.5 ± 0.4	26 ± 8	0.17 ± 0.07
Lys205Ala	3.1 ± 0.1	85 ± 10	0.037 ± 0.005
Leu268Ala	6.2 ± 0.2	280 ± 30	0.022 ± 0.003
His334Met	2.0 ± 0.1	61 ± 10	0.033 ± 0.007
Arg405Ala	14 ± 2	290 ± 75	0.048 ± 0.019
Thr271Ala	4.0 ± 0.2	75 ± 11	0.05 ± 0.01

[a] Chorismate mutase activity was determined at pH 7.5 in the absence of Mg^{2+}. Reactions were performed in 100 mM Tris-HCl buffer at 37 °C as described in the text. In the case of the mutant enzymes, the addition of Mg^{2+} had no effect on the catalyzed reaction.

pH 8 the primary product is salicylate. Small amounts of isochorismate can be detected in the HPLC chromatograms of reactions performed at pH 8, as well as in the NMR spectra of reaction mixtures containing MbtI and chorismate (see below), and at this pH MbtI converts isochorismate to salicylate with a k_{cat}/K_m value of 0.81 μM^{-1} min^{-1}. Since the k_{cat}/K_m value for salicylate synthesis at pH 8 is 0.5 μM^{-1} min^{-1}, these data suggest that isochorismate is a kinetically competent intermediate in the conversion of chorismate to salicylate catalyzed by MbtI. The k_{cat} value of 2.8 min^{-1} for the conversion of chorismate to salicylate is more than 2 orders of magnitude smaller than the AS activity of the MST family member AS-sm (558 min^{-1}) (*18*) but is comparable to the salicylate synthase activity of Irp9 (8 min^{-1}) from *Yersinia enterocolitica* (*9*). In the absence of Mg^{2+}, WT MbtI displays chorismate mutase activity at pH 7−8 and converts chorismate to prephenate at a rate comparable to the Mg^{2+}-dependent activities. Thus, the chorismate mutase activity of WT MbtI is substantially less efficient compared to other chorismate mutases from *M. tuberculosis* (*33*). In contrast to the WT enzyme, only chorismate mutase activity could be detected in the Lys205Ala, Leu268Ala, Thr271Ala, His334Met, and Arg405Ala MbtI mutants in both the presence and absence of Mg^{2+}, while no activity could be detected for the Glu252Gln mutant. The observation that one MbtI mutant displays no chorismate mutase activity, together with the 10-fold variation in K_m values measured for the chorismate mutase activities of WT and mutant MbtIs (Table 3), strongly suggests that the observed chorismate mutase activity is not the result of a contaminating enzyme. This conclusion is supported by the observation that further purification of each protein using anion exchange chromatography had no impact on the measured activities.

Sequence Comparison. A BLAST analysis reveals that the C-terminus of MbtI contains the consensus sequence shared by other chorismate-binding enzymes such as AS and isochorismate synthase. The structure of the *S. marcescens* AS has been determined, and MbtI is 31% identical and 45% similar to the chorismate-binding (TrpE) subunit of this enzyme. MbtI superimposes on the AS-sm ligand structure with a rms deviation of 2.5 Å, and, at a distance of up to 6 Å from the bound ligands, 20 out of 26 amino acids are conserved in MbtI. When compared with other MST enzymes, there are no conserved active site residues that are unique to pyruvate eliminating enzymes such as MbtI and AS-sm that could assume a role in the originally proposed pyruvate elimination mechanisms (Figure 4). In addition, none of the 6 residues that differ between the MbtI and AS-sm active sites have polar side chains directly contacting the ligand, while only MbtI Lys205 and Leu268 are likely to be directly involved in catalysis. By analogy to our studies on MenF (*8*), we propose that Lys205 activates a water molecule for attack at the C2 of chorismate (*34*) and the proximity of the backbone carbonyl of Leu268 to the essential Glu252 and C4 hydroxyl suggests that Leu268 is involved in recognition and elimination of the C4 hydroxyl. MbtI Arg417 is the only other nonidentical polar residue within 6 Å of the substrate and directly precedes a conserved XAGAG sequence that recognizes both the C1 ring carboxylate and the pyruvate in the AS-sm structure. Salicylate synthases conserve either an Arg or Gln at this position and the homologous AS-sm residue is Gln481. In contrast, isochorismate synthases have a preference for a conserved aromatic residue at this position, and thus variability in this motif may correlate with pyruvate elimination. During the preparation of this manuscript, the structure of the salicylate synthase, Irp9, from *Yersinia enterocolitica*, was reported (*21*). MbtI is 36% identical and 56% similar to Irp9, and the two enzymes have an rms deviation of 2.1 Å. The Irp9 structure was solved in complex with Mg^{2+}, salicylate, and pyruvate, and 27 of 28 residues within 6 Å of the bound product are conserved in MbtI. MbtI Arg417 is replaced by Gln402 in Irp9.

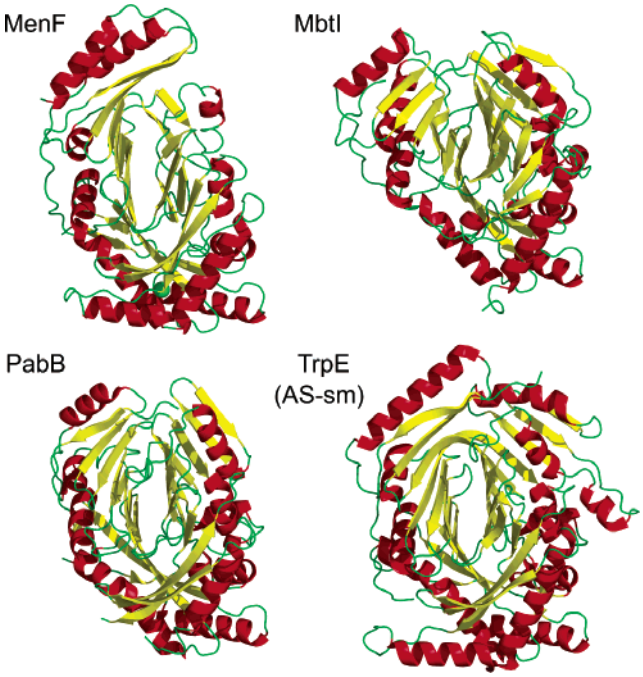

FIGURE 5: Structural conservation in the MST family. All members of the MST family contain the two domain twisting β-sandwich motif first characterized by Knochel et al. (*10*). MbtI, MenF, PabB, and AS-sm are rendered with the α-helices in red and β-strands in yellow. For clarity, only single subunits are shown for MenF, PabB, and As-sm. The figure was created using pymol (*49*).

Structure of MbtI. MbtI crystallizes as a monomer and has a two domain β-sandwich fold shared by all members of the MST family (Figure 5) (*8*, *10*−*12*, *35*). In the apo MbtI structure, no density was observed for the N-terminal 16 residues as well as for two active site sequence stretches (Arg276−Asp286 and Glu328−Gly330) that show significant conformational changes in homologous enzymes upon ligand binding. In aminodeoxyisochorismate synthase (PabB) (*35*) the homologous residues are similarly disordered (PDB

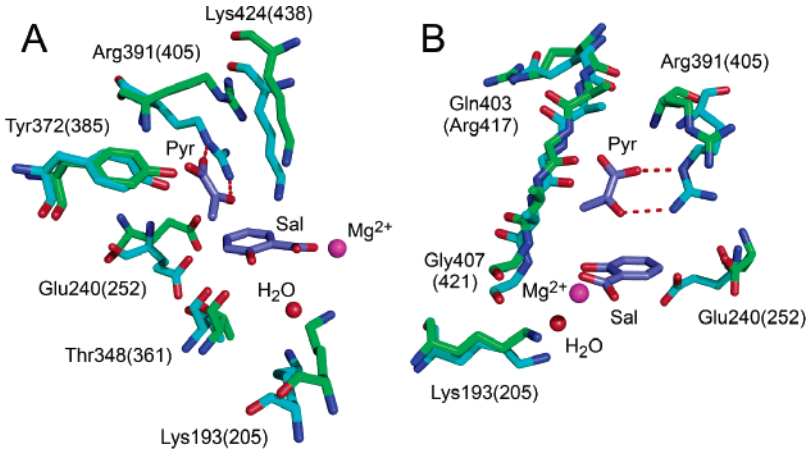

FIGURE 6: Superposition of the MbtI and Irp9 active sites. The apo MbtI active site is more open than that of the ligand-bound Irp9 structure. Two views are shown labeled A and B. Irp9 residues are in cyan while the corresponding residues in MbtI are colored green and numbered in parentheses. The pyruvate and salicylate ligands bound to Irp9 are colored slate (*49*). The figure was created using Pymol (*49*).

ID 1K0G) and become partially ordered (PDB ID 1K0E) when formate is bound at the position normally occupied by pyruvate in other MST structures. In MbtI, residues Thr271−Leu274 are located adjacent to the missing residues and form a small helix that partially obstructs the active site. Upon ligand binding this helix must move to accommodate the substrate. Apart from this helix, the structure of MbtI is very similar to that of the salicylate synthase Irp9. Small differences in the positions of active site residues between the two enzymes can be accounted for by the presence of salicylate and pyruvate in the Irp9 active site. Figure 6 contains a superposition of selected residues from MbtI and Irp9 highlighting the similarity between the two enzymes. Finally, as observed in our recent MenF structure (*8*), MbtI has a main chain aromatic amino acid in a position homologous to the regulatory Trp in other MST enzymes. MbtI is Trp insensitive, and superposition shows that MbtI Tyr48 occupies the position of the regulatory Trp in the As-sm structure.

NMR Spectroscopy. The reaction of MbtI with chorismate was monitored by ^{1}H NMR spectroscopy at pD 7.8 (Figure 7). After a short time, small peaks assigned to isochorismate can be observed in the spectrum followed by the slower formation of salicylate and pyruvate. Of particular importance is the line shape of the peak assigned to the methyl group of pyruvate at 2.38 ppm. The pyruvate methyl resonance is a singlet, supporting the direct transfer of a proton from the isochorismate C2 carbon to the enolpyruvyl side chain. If the proton acquired by the pyruvate methyl group during the elimination reaction had been derived from solvent, then a triplet would have been expected for this resonance (CH2D).

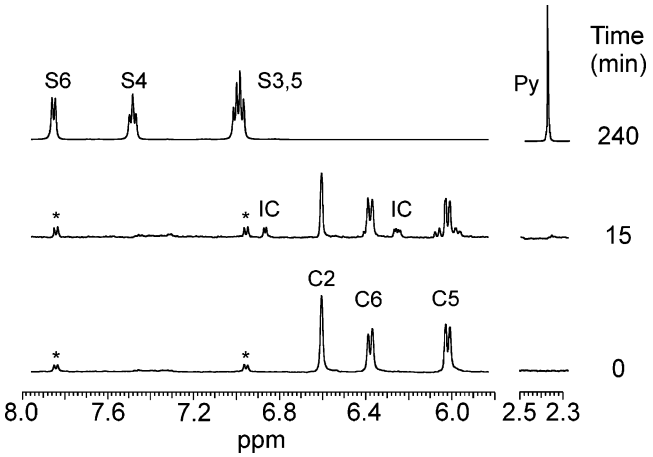

FIGURE 7: ^{1}H NMR spectra of chorismate in the absence and presence of MbtI. ^{1}H NMR spectra of chorismate (2 mM) were obtained in D_2O buffer (20 mM potassium phosphate, 5 mM $MgCl_2$ pD 7.8) in the absence and presence of WT MbtI (25 μM) at 30 °C. Two regions of the spectrum are shown. Resonances arising from chorismate (C2, C5, and C6), isochorismate (IC), and salicylate (S3,5, S4 and S6) are observed in the region from 6.0 to 8.0 ppm, while the resonance associated with the pyruvate methyl group (Py) can be observed between 2.3 and 2.5 ppm at 2.38 ppm. The resonance arising from the pyruvate methyl group is a singlet, consistent with the direct transfer of a proton from the C2 carbon of isochorismate to the enolpyruvyl group. Features marked with a * are due to a contaminant in the chorismate.

DISCUSSION

Bacteria require iron for growth and consequently produce iron-chelating molecules called siderophores that very efficiently scavenge iron from the environment. In *M. tuberculosis* the siderophore is mycobactin, and the biosynthesis of this molecule is under the transcriptional control of the iron-dependent regulator IdeR (*36*). Like other siderophores, an initial step in the biosynthesis of mycobactin is the conversion of chorismate to salicylate (*1*, *4*). In general, this is accomplished either by a single salicylate synthase enzyme or by a pair of enzymes, an isochorismate synthase and an isochorismate pyruvate lyase, acting in concert. In *M. tuberculosis*, the core of the mycobactin molecule is synthesized by enzymes encoded by the *mbt* operon which contains ten genes including *mbtI*. Our studies show that MbtI catalyzes the Mg^{2+} dependent formation of salicylate from chorismate, consistent with the observation that *M. tuberculosis* lacks homologues of the isochorismate pyruvate lyase enzyme that would be required for the subsequent conversion of isochorismate to salicylate. Thus MbtI catalyzes both the isomerization of chorismate to isochorismate and the subsequent elimination of pyruvate from isochorismate.

MbtI is a member of a family of chorismate-binding enzymes that catalyze distinct reactions on a conserved

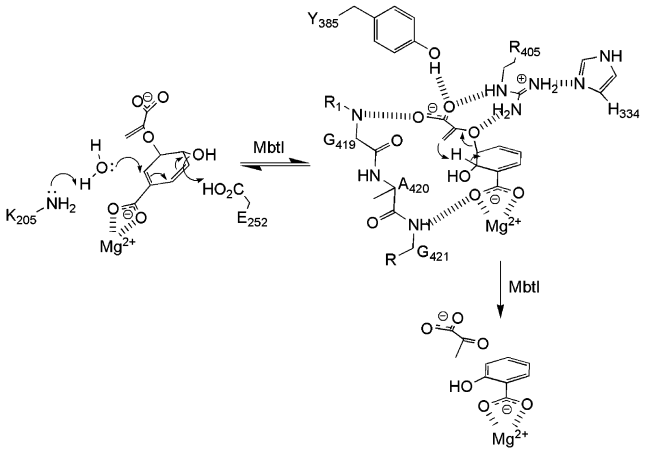

FIGURE 8: The proposed MbtI reaction mechanism. Lys205 activates a water molecule for attack at the C2 carbon of chorismate resulting in an S_N2'' reaction in which water is eliminated from the C4 carbon of chorismate upon protonation by Glu 252. The ether bond of the isochorismate intermediate, bound in a twisted boat conformation, is cleaved concomitant with transfer of the C2 proton to the *re* face of the pyruvate. We propose that this mechanism is valid for the entire MST family.

structural template (*5*). A mechanism for isomerization and substitution within this enzyme family has recently been proposed (*34*), while pyruvate elimination has generally been thought to occur via acid/base catalysis utilizing one or more active site residues (*12*, *35*). In the present study we have determined the structure of MbtI, and together, with the observation that MbtI catalyzes the formation of prephenate, as well as isochorismate and salicylate, we propose a mechanism for pyruvate elimination applicable to the entire MST family.

Isochorismate and Salicylate Synthase Activities. MbtI (Rv2386c) is annotated in the *M. tuberculosis* genome as an isochorismate synthase and is 28% identical and 46% similar to MenF the isochorismate synthase from *E. coli*. At pH 7 MbtI does indeed demonstrate isochorismate synthase activity, but as the pH is raised above 7.5 salicylate becomes the primary product. In addition, at pH 8 MbtI can utilize isochorismate as a substrate for salicylate production and the kinetic data show that isochorismate is a kinetically competent intermediate on the reaction pathway. As observed for other homologues in the MST enzyme family, the isochorismate and salicylate synthase activity of MbtI is Mg^{2+} dependent and analysis of the structural data reveals that the Mg^{2+} is coordinated by two conserved acidic residues, Glu297 and Glu434, as well as the C1 carboxylate of chorismate. The structural data also shows that Lys205 is appropriately positioned to assist in the attack of water at the chorismate C2 carbon for the isomerization reaction and that Glu252 could provide acid catalysis for the elimination of the hydroxyl group from C4 carbon (Figure 8).

Accumulation of isochorismate at pH values below 7.5 can be explained by the ionization of an active site residue required for the subsequent elimination of pyruvate from isochorismate. Currently we do not know the identity of this ionizable residue, although His334 likely plays a key role in positioning the isochorismate pyruvate side chain in the active site (see below). More intriguingly, it is not immediately apparent why isochorismate is the favored product at pH values below 7.5 given that the intracellular pH of the bacterium is thought to be around 7.0 (*37*) and that salicylate and not isochorismate is required for mycobactin biosynthesis. One possibility is that interactions within the mycobacterium, for example with MbtA, the next enzyme in the mycobactin biosynthetic pathway, control whether isochorismate or salicylate is the product of the MbtI reaction. Thus MbtI may function as both a salicylate synthase and an isochorismate synthase in vivo. In this regard, while transcription of the *mbt* operon is regulated by iron, it is possible that there is some basal expression of MbtI even in the presence of iron and that isochorismate synthesis is a normal function of the protein. Along these lines, so far we have been unable to demonstrate that EntC, the other isochorismate synthase annotated in the *M. tuberculosis* genome, is able to synthesize isochorismate (unpublished data). This is of importance given the requirement of isochorismate for menaquinone biosynthesis (*38*).

Pyruvate Elimination. Acid−Base Catalysis? The product bound structure of AS-sm (*12*) and an AS-sm His398Met mutant that accumulated the ADIC intermediate (*18*) support a mechanism for pyruvate elimination in which His398 (His334 in MbtI) abstracts the C2 isochorismate proton (Figure 4). Parsons et al. have also proposed an acid/base-catalyzed elimination mechanism in which abstraction of the C2 proton by an unidentified base is either followed by, or concerted with, protonation of the enolpyruvyl side chain by residues homologous to either MbtI Glu252 or Tyr385 (Figure 4). However, a role for either residue in acid catalysis has been questioned by mutagenesis data (*21*, *39*). In addition, a comparison of the available MST crystal structures (*8*, *10*−*12*, *35*) and more than 1000 MST sequences reveals that there are no active site residues that directly contact the ligand and that are unique to the pyruvate-eliminating salicylate or anthranilate synthases. Thus, these enzymes must utilize an alternative strategy for pyruvate elimination, and a clue regarding how this is accomplished was provided by the observation that MbtI has chorismate mutase activity.

Chorismate Mutase Activity. Our attempts to explore the catalytic mechanism of MbtI, and, in particular, to identify residue(s) responsible for controlling elimination of the pyruvate group from isochorismate, led to the generation and characterization of a series of active site mutants. In almost every case (Lys205Ala, Leu268Ala, Thr271Ala, His334Met, and Arg405Ala) these MbtI mutants had chorismate mutase activity, and we subsequently discovered that WT MbtI displayed chorismate mutase activity in the absence of Mg^{2+}. In order to explain this observation, we propose that chorismate is bound to MbtI in a diaxial conformation that is optimized for isomerization and elimination, and from which prephenate can be also be formed. Hilvert and coworkers have extensively studied the uncatalyzed rearrangement of chorismate and isochorismate (*14*, *40*) (Figure 2), and demonstrated that the nonenzymatic fates of the molecules depend upon the orientation of their enolpyruvyl side chains. Specifically, it was shown that the elimination of pyruvate from chorismate and isochorismate to give *p*-hydroxybenzoate and salicylate, respectively, proceeded via a concerted pericyclic mechanism in which the respective C4 and C2 protons are transferred to the enolpyruvyl side chain. A similar mechanism was subsequently proposed for the isochorismate pyruvate lyase, PchB (*15*). Like MbtI,

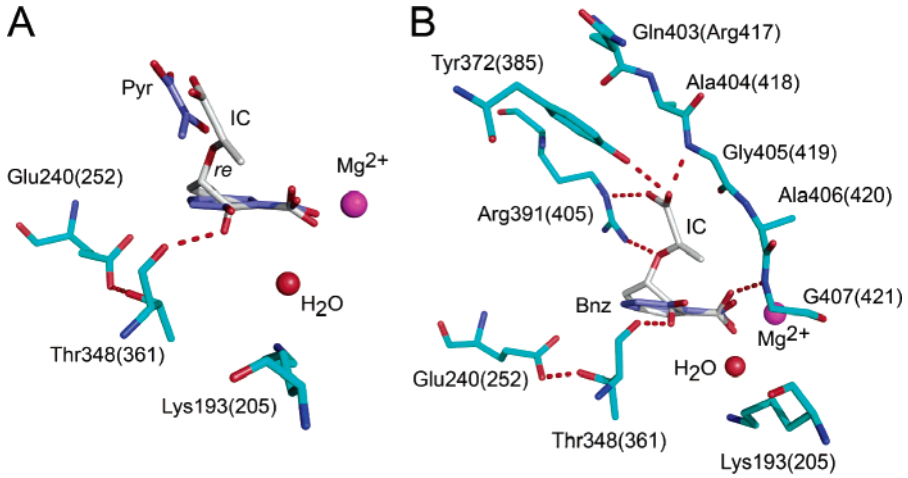

FIGURE 9: Isochorismate docked into the Irp9 and MbtI active sites. Isochorismate (IC, gray) was superimposed on the salicylate ligand (slate) from the Irp9 structure. The enolpyruvyl side chain of isochorismate has been oriented to match the position of the bound pyruvate ligand (slate). The view in panel A shows the bound pyruvate ligand while in panel B the pyruvate has been removed and postulated interactions between isochorismate (IC) and active site residues are shown. The residues shown in cyan are from Irp9 while numbers and labels in parentheses refer to the corresponding residues in MbtI. The figure was created using pymol (*49*).

PchB also has chorismate mutase activity suggesting that chorismate can bind to the enzyme in an orientation that facilitates a sigmatropic rearrangement (*16*). Hilvert and coworkers demonstrated that PchB catalyzed the elimination of pyruvate from isochorismate via a sigmatropic mechanism in which the C2 proton of isochorismate is transferred to the pyruvate (*13*, *15*). If a similar reaction mechanism is utilized by MbtI, then we must consider the orientation of the substrate in the active site and stereochemistry of the reaction.

A Sigmatropic Elimination Mechanism. Stereochemistry, Model Building, and NMR Spectroscopy. The steric course of the reaction catalyzed by AS has been previously investigated by Asano et al. (*41*). Using selectively deuterated and tritiated chorismate, it was shown that the pyruvate side chain is stereospecifically protonated on its *re* face during the synthesis of anthranilate by AS-sm (*41*). Assuming that the stereochemistry of the MbtI reaction mirrors that observed for As-sm, then intramolecular proton transfer within the isochorismate molecule requires that the *re* face of the enolpyruvyl group face C2. Indeed, superposition of isochorismate on the salicylate ligand in the active site of Irp9 (*21*) and alignment of the side chain to match the position of the bound pyruvate suggests that the substrate can adopt a twisted boat conformation (*40*) in which the *re* face of the enolpyruvyl side chain is oriented toward the isochorismate C2 carbon (Figure 9). In this conformation, the only labile proton accessible to the *re* face of the pyruvate side chain, apart from that of the substrate, corresponds to the hydroxyl group of Tyr449 (MbtI Tyr385) which is already hydrogen bonded to the pyruvate carboxylate. This tyrosine is highly conserved throughout the MST family in both pyruvate retaining and eliminating enzymes, and, as described above, mutagenesis data suggests that this residue is unlikely to function as an acid in the reaction (*21*, *39*).

Direct experimental support for intramolecular proton transfer was subsequently provided by monitoring the MbtI-catalyzed formation of pyruvate from chorismate in D_2O buffer using ^1H NMR spectroscopy. Figure 7 shows that the resonance at 2.38 ppm, assigned to the methyl group of the pyruvate formed in this reaction, is a singlet, indicating that solvent deuterium was not incorporated into the product during pyruvate elimination. Although an enzyme residue could in principle abstract the C2-H isochorismate proton and then transfer it to the enolpyruvyl side chain without solvent exchange occurring, the simplest explanation is that the C2-H proton has been directly transferred to the enolpyruvyl group.

Returning to the chorismate mutase activity of MbtI, chorismate has to be bound in a conformation such that the enolpyruvyl group can approach the C1 substrate carbon. This can occur by slight changes in the orientation of the side chain in the diaxial twisted boat conformation depicted in Figure 9 in which the enolpyruvyl side chain forms hydrogen bonds with Tyr372, Arg391, and Gly405. It is interesting to note that AroH class chorismate mutases similarly use Arg and Tyr residues to position the pyruvate side chain of the substrate (*42*). If prephenate formation does indeed occur from a diaxial twisted boat chorismate conformation, then this contrasts with the normally accepted mechanism for chorismate mutases in which the reaction occurs from the energetically more favorable chair conformation (*41*, *43*). Although this is an intriguing possibility, it must be noted that WT MbtI catalyzes prephenate formation only in the absence of Mg^{2+} while the model presented in Figure 9 is based on the Mg^{2+}-bound structure of Irp9. Thus, we cannot rule out the possibility that chorismate adopts a substantially different conformation to that shown in Figure 9 in the absence of Mg^{2+} and that it is this conformation that leads to prephenate formation. Further studies will be required to differentiate between these possibilities.

Role of Mg^{2+}. Chorismate mutase activity is present only in WT MbtI in the absence of Mg^{2+} or in selected mutants. All chorismate binding enzymes that are not members of the MST family, including chorismate mutase (*42*), chorismate pyruvate lyase (*44*), and isochorismate pyruvate lyase (*16*), use an arginine to coordinate the C1 carboxylate of their respective substrates. These enzymes are also Mg^{2+} independent. Computational studies by Marti et al. (*45*) of the *Bacillus subtilis* chorismate mutase (BsCM) show that the interaction between the C1 carboxylate of chorismate and BsCM Arg116 are weakened upon going from the

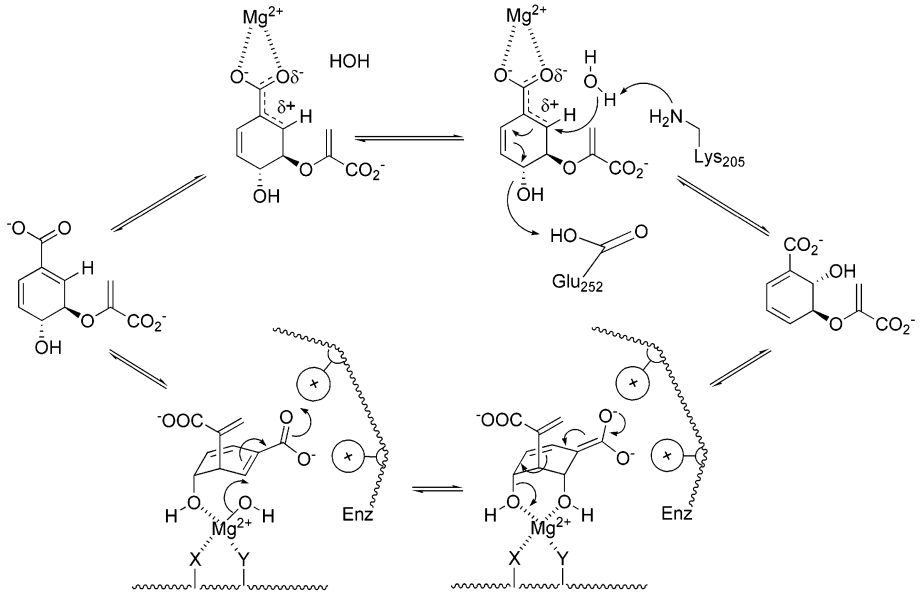

FIGURE 10: Interactions that increase the electrophilicity of the chorismate C2 carbon. In the MST enzyme family Mg^{2+} binding may generate a partial positive charge at the C2 of chorismate, activating it for nucleophilic attack at that position according to the model proposed by He et al. (*34*). This is shown in the upper reaction path. This situation is analogous to the lower reaction path, originally proposed by Walsh et al. (*20*), in which the Mg^{2+} was proposed to coordinate both the incoming nucleophile and departing C4 hydroxyl. Two positively charged active site residues were predicted to take the place of the divalent Mg^{2+}ion, and stabilize a dienolate intermediate. The structures in the lower reaction path are adapted from Figures 17 and 20 in ref *20*.

reactant to the transition state. This suggests that interactions with the ring carboxylate are not essential for the chorismate to prephenate isomerization. In the MST enzymes Mg^{2+} could potentially be involved in ligand activation. He et al.'s general mechanism for the MST family involves attack at the C2 carbon of chorismate by an exogenous or main chain nucleophile (*34*). Ligand polarization by Mg^{2+}, as shown in Figure 10, would generate a partial positive charge at the C2 position, facilitating nucleophilic attack at that position. This is similar to the proposal by Walsh et al. (*20*) in which positively charged active site residues perform an analogous role to the Mg^{2+} as part of an SN2″ Michael addition/elimination sequence (Figure 10). We propose that chorismate is bound to MbtI in a conformation that can partition either to isochorismate or to prephenate. In the WT enzyme activation of C2 by Mg^{2+} results in isochorismate formation while in the absence of Mg^{2+} prephenate is the preferred product. The two reaction pathways are finely balanced, and thus mutations that perturb isomerization, for example mutation of the catalytic base Lys205, result in prephenate formation.

CONCLUSION

In the present study we demonstrate that MbtI, the first enzyme in the mycobactin biosynthetic operon, is able to catalyze the formation of isochorismate, salicylate, and prephenate from chorismate. We hypothesize that chorismate binds to the enzyme in a diaxial conformation that can form isochorismate or prephenate. Isochorismate is only formed when Mg^{2+} is bound to the WT enzyme, and we postulate that the role of Mg^{2+} is to increase the electrophilicity of the chorismate C2 carbon. Perturbation of the isomerization reaction either by removing Mg^{2+} or by mutation of residues surrounding the ligand leads to the formation of prephenate. In addition, we propose that pyruvate is eliminated from isochorismate in a sigmatropic reaction mechanism in which the ligand is bound to the enzyme in a twisted boat conformation such that the *re* face of the enolpyruvyl side chain is oriented toward C2. This isochorismate pyruvate lyase activity of the isolated enzyme is pH dependent, and we speculate that the ionization state of one or more active site residues, such as His334, may control the affinity of isochorismate for the enzyme and/or subtle positioning of the side chain required for the sigmatropic reaction. Further studies utilizing isotopically labeled chorismate and isochorismate molecules will shed further light on these possibilities.

At present it is not known which reactions MbtI catalyzes in vivo. Salicylate is required for mycobactin biosynthesis, and it is possible that this is the only intracellular product formed by MbtI. If so, then product formation must be regulated within the cell by, for example, interactions with other enzymes in the biosynthetic pathway. Alternatively, MbtI may also function as an isochorismate synthase and be involved in the biosynthesis of menaquinone. In addition, while the intracellular concentration of Mg^{2+} is unknown, it seems less likely that MbtI has an important role in prephenate formation given the high relative activities of other characterized chorismate mutases from *M. tuberculosis*. Nevertheless, the observation that MbtI possesses chorismate mutase activity provides mechanistic insight into the reaction mechanism and also suggests attractive strategies for inhibitor design. In this regard, it is worth noting that antimicrobial agents that are directed at siderophore biosynthesis or that disrupt the flux of chorismate have promising applications in the treatment of numerous pathogens such as *M. tuberculosis* (*4*, *33*, *46*−*48*).

ACKNOWLEDGMENT

We thank Dr. Peter Kast of the ETH for providing *E. coli* strain KA12 which was used as a source of chorismate.

Atomic coordinates have been deposited in the Protein Data Bank with access code 2I6Y.

REFERENCES

1. Quadri, L. E., Sello, J., Keating, T. A., Weinreb, P. H., and Walsh, C. T. (1998) Identification of a *Mycobacterium tuberculosis* gene cluster encoding the biosynthetic enzymes for assembly of the virulence-conferring siderophore mycobactin, *Chem. Biol. 5*, 631−645.
2. De Voss, J. J., Rutter, K., Schroeder, B. G., and Barry, C. E., III (1999) Iron acquisition and metabolism by mycobacteria, *J. Bacteriol. 181*, 4443−4451.
3. De Voss, J. J., Rutter, K., Schroeder, B. G., Su, H., Zhu, Y., and Barry, C. E., III (2000) The salicylate-derived mycobactin siderophores of *Mycobacterium tuberculosis* are essential for growth in macrophages, *Proc. Natl. Acad. Sci. U.S.A. 97*, 1252−1257.
4. Crosa, J. H., and Walsh, C. T. (2002) Genetics and assembly line enzymology of siderophore biosynthesis in bacteria, *Microbiol. Mol. Biol. Rev. 66*, 223−249.
5. Kozlowski, M. C., Tom, N. J., Seto, C. T., Sefler, A. M., and Bartlett, P. A. (1995) Chorismate-utilizing enzymes isochorismate synthase, anthranilate synthase, and p-aminobenzoate synthase: mechanistic insight through inhibitor design, *J. Am. Chem. Soc. 117*, 2128−2140.
6. Dahm, C., Muller, R., Schulte, G., Schmidt, K., and Leistner, E. (1998) The role of isochorismate hydroxymutase genes entC and menF in enterobactin and menaquinone biosynthesis in Escherichia coli, *Biochim. Biophys. Acta 1425*, 377−386.
7. Daruwala, R., Bhattacharyya, D. K., Kwon, O., and Meganathan, R. (1997) Menaquinone (vitamin K2) biosynthesis: overexpression, purification, and characterization of a new isochorismate synthase from Escherichia coli, *J. Bacteriol. 179*, 3133−3138.
8. Kolappan, S., Zwahlen, J., Zhou, R., Truglio, J., Tonge, P. J., and Kisker, C. (2006) Lysine 190 is the Catalytic Base in MenF, the Menaquinone-Specific Isochorismate Synthase from *Escherichia coli*: Implications for an Enzyme Family, *Biochemistry 45*, 946−953.
9. Kerbarh, O., Ciulli, A., Howard, N. I., and Abell, C. (2005) Salicylate biosynthesis: overexpression, purification, and characterization of Irp9, a bifunctional salicylate synthase from *Yersinia enterocolitica*, *J. Bacteriol. 187*, 5061−5066.
10. Knochel, T., Ivens, A., Hester, G., Gonzalez, A., Bauerle, R., Wilmanns, M., Kirschner, K., and Jansonius, J. N. (1999) The crystal structure of anthranilate synthase from Sulfolobus solfataricus: functional implications, *Proc. Natl. Acad. Sci. U.S.A. 17*, 9479−9484.
11. Morollo, A. A., and Eck, M. J. (2001) Structure of the cooperative allosteric anthranilate synthase from Salmonella typhimurium, *Nat. Struct. Biol. 8*, 243−247.
12. Spraggon, G., Kim, C., Nguyen-Huu, X., Yee, M. C., Yanofsky, C., and Mills, S. E. (2001) The structures of anthranilate synthase of Serratia marcescens crystallized in the presence of (i) its substrates, chorismate and glutamine, and a product, glutamate, and (ii) its end-product inhibitor, L-tryptophan, *Proc. Natl. Acad. Sci. U.S.A.* 98, 6021−6026.
13. DeClue, M. S., Baldridge, K. K., Kunzler, D. E., Kast, P., and Hilvert, D. (2005) Isochorismate pyruvate lyase: A pericyclic reaction mechanism?, *J. Am. Chem. Soc. 127*, 15002−15003.
14. Wright, S. K., DeClue, M. S., Mandal, A., Lee, L., Wiest, O., Cleland, W. W., and Hilvert, D. (2005) Isotope Effects on the Enzymatic and Nonenzymatic Reactions of Chorismate, *J. Am. Chem. Soc. 127*, 12957−12964.
15. Kunzler, D. E., Sasso, S., Gamper, M., Hilvert, D., and Kast, P. (2005) Mechanistic insights into the isochorismate pyruvate lyase activity of the catalytically promiscuous PchB from combinatorial mutagenesis and selection, *J. Biol. Chem. 280*, 32827−32834.
16. Gaille, C., Kast, P., and Haas, D. (2002) Salicylate biosynthesis in *Pseudomonas aeruginosa*. Purification and characterization of PchB, a novel bifunctional enzyme displaying isochorismate pyruvate-lyase and chorismate mutase activities, *J. Biol. Chem. 277*, 21768−21775.
17. Gaille, C., Reimmann, C., and Haas, D. (2003) Isochorismate synthase (PchA), the first and rate-limiting enzyme in salicylate biosynthesis of *Pseudomonas aeruginosa*, *J. Biol. Chem. 278*, 16893−16898.
18. Morollo, A. A., and Bauerle, R. (1993) Characterization of composite aminodeoxyisochorismate synthase and aminodeoxyisochorismate lyase activities of anthranilate synthase, *Proc. Natl. Acad. Sci. U.S.A. 90*, 9983−9987.
19. Tso, J. Y., and Zalkin, H. (1981) Chemical Modifications Of *Serratia-Marcescens* Anthranilate Synthase Component-I, *J. Biol. Chem. 256*, 9901−9908.
20. Walsh, C. T., Liu, J., Rusnak, F., and Sakaitani, M. (1990) Molecular studies on enzymes in chorismate metabolism and the enterobactin biosynthetic pathway, *Chem. Rev. 90*, 1105−1129.
21. Kerbarh, O., Chirgadze, D. Y., Blundell, T. L., and Abell, C. (2006) Crystal structures of *Yersinia enterocolitica* salicylate synthase and its complex with the reaction products salicylate and pyruvate, *J. Mol. Biol. 357*, 524−534.
22. Payne, R. J., Kerbarh, O., Miguel, R. N., Abell, A. D., and Abell, C. (2005) Inhibition studies on salicylate synthase, *Org. Biomol. Chem. 3*, 1825−1827.
23. Grisostomi, C., Kast, P., Pulido, R., Huynh, J., and Hilvert, D. (1997) Efficient in Vivo Synthesis and Rapid Purification of Chorismic Acid Using an Engineered *Escherichia coli* Strain, *Bioorg. Chem. 25*, 297−305.
24. Liu, J., Quinn, N., Berchtold, G. A., and Walsh, C. T. (1990) Overexpression, purification, and characterization of isochorismate synthase (EntC), the first enzyme involved in the biosynthesis of enterobactin from chorismate, *Biochemistry 29*, 1417−1425.
25. Rusnak, F., Liu, J., Quinn, N., Berchtold, G. A., and Walsh, C. T. (1990) Subcloning of the enterobactin biosynthetic gene entB: expression, purification, characterization and substrate specificity of isochorismatase, *Biochemistry 29*, 1425−1435.
26. Otwinowski, Z., and Minor, W. (1997) Processing of X-ray Diffraction Data Collected in Oscillation Mode, *Methods Enzymol. 276*, 307−326.
27. Terwilliger, T. C., and Berendzen, J. (1999) Automated MAD and MIR structure solution, *Acta Crystallogr. D 55*, 849−861.
28. Terwilliger, T. C. (2000) Maximum-likelihood density modification, *Acta Crystallogr. D 56*, 965−972.
29. Cowtan, K. (1994) An automated procedure for phase improvement by density modification, *Joint CCP4 and ESF-EACBM Newsletter on Protein Crystallography 31*, 34−38.
30. Jones, T. A., Zou, J. Y., Cowan, S. W., and Kjeldgaard, M. (1991) Improved methods for building protein models in electron density maps and the location of errors in these models, *Acta Crystallogr. A47*, 110−119.
31. Bailey, S. (1994) The Ccp4 Suite—programs for protein crystallography, *Acta Crystallogr. D50*, 760−763.
32. Laskowski, R. A., MacArthur, M. W., Moss, D. S., and Thornton, J. M. (1993) The lattice constant of a nonperfect crystal measured by X-ray diffraction, *J. Appl. Crystallogr. 26*, 280−283.
33. Sasso, S., Ramakrishnan, C., Gamper, M., Hilvert, D., and Kast, P. (2005) Characterization of the secreted chorismate mutase from the pathogen *Mycobacterium tuberculosis*, *FEBS J. 272*, 375−389.
34. He, Z., Stigers Lavoie, K. D., Bartlett, P. A., and Toney, M. D. (2004) Conservation of mechanism in three chorismate-utilizing enzymes, *J. Am. Chem. Soc. 126*, 2378−2385.
35. Parsons, J. F., Jensen, P. Y., Pachikara, A. S., Howard, A. J., Eisenstein, E., and Ladner, J. E. (2002) Structure of *Escherichia coli* aminodeoxychorismate synthase: architectural conservation and diversity in chorismate-utilizing enzymes, *Biochemistry 41*, 2198−2208.
36. Rodriguez, G. M., Voskuil, M. I., Gold, B., Schoolnik, G. K., and Smith, I. (2002) ideR, An essential gene in *Mycobacterium tuberculosis*: role of IdeR in iron-dependent gene expression, iron metabolism, and oxidative stress response, *Infect. Immun. 70*, 3371−3381.
37. Zhang, Y., Scorpio, A., Nikaido, H., and Sun, Z. (1999) Role of acid pH and deficient efflux of pyrazinoic acid in unique susceptibility of *Mycobacterium tuberculosis* to pyrazinamide, *J. Bacteriol. 181*, 2044−2049.
38. Truglio, J. J., Theis, K., Feng, Y., Gajda, R., Machutta, C., Tonge, P. J., and Kisker, C. (2003) Crystal structure of *Mycobacterium tuberculosis* MenB, a key enzyme in vitamin K2 biosynthesis, *J. Biol. Chem. 278*, 42352−42360.
39. Kanno, T., Komatsu, A., Kasai, K., Dubouzet, J. G., Sakurai, M., Ikejiri-Kanno, Y., Wakasa, K., and Tozawa, Y. (2005) Structure-Based in Vitro Engineering of the Anthranilate Synthase, a Metabolic Key Enzyme in the Plant Tryptophan Pathway, *Plant Physiol. 138*, 2260−2268.

40. DeClue, M. S., Baldridge, K. K., Kast, P., and Hilvert, D. (2006) Experimental and computational investigation of the uncatalyzed rearrangement and elimination reactions of isochorismate, *J. Am. Chem. Soc. 128*, 2043−2051.
41. Asano, Y., Lee, J. J., Shieh, T. L., Spreafico, F., Kowal, C., and Floss, H. G. (1985) Steric course of the reactions catalyzed by 5-enolpyruvylshikimate-3-phosphate synthase, chorismate mutase, and anthranilate synthase, *J. Am. Chem. Soc. 107*, 4314−4320.
42. Chook, Y. M., Ke, H., and Lipscomb, W. N. (1993) Crystal structures of the monofunctional chorismate mutase from *Bacillus subtilis* and its complex with a transition state analog, *Proc. Natl. Acad. Sci. U.S.A. 90*, 8600−8603.
43. Sogo, S. G., Widlanski, T. S., Hoare, J. H., Grimshaw, C. E., Berchtold, G. A., and Knowles, J. R. (1984) Stereochemistry of the Rearrangement of Chorismate to Prephenate: Chorismate Mutase Involves a Chair Transition State, *J. Am. Chem. Soc. 106*, 2701−2703.
44. Gallagher, D. T., Mayhew, M., Holden, M. J., Howard, A., Kim, K. J., and Vilker, V. L. (2001) The crystal structure of chorismate lyase shows a new fold and a tightly retained product, *Proteins 44*, 304−311.
45. Marti, S., Andres, J., Moliner, V., Silla, E., Tunon, I., and Bertran, J. (2004) A comparative study of claisen and cope Rearrangements catalyzed by chorismate mutase. An insight into enzymatic efficiency: Transition state stabilization or substrate preorganization?, *J. Am. Chem. Soc. 126*, 311−319.
46. Doyle, E. A., and Lambert, K. N. (2003) Meloidogyne javanica chorismate mutase 1 alters plant cell development, *Mol. Plant-Microbe Interact. 16*, 123−131.
47. Sassetti, C. M., Boyd, D. H., and Rubin, E. J. (2003) Genes required for mycobacterial growth defined by high density mutagenesis, *Mol. Microbiol. 48*, 77−84.
48. Ferreras, J. A., Ryu, J. S., Di Lello, F., Tan, D. S., and Quadri, L. E. N. (2005) Small-molecule inhibition of siderophore biosynthesis in Mycobacterium tuberculosis and Yersinia pestis, *Nat. Chem. Biol. 1*, 29−32.
49. DeLano, W. L. The PyMOL Molecular Graphics System (2002) on World Wide Web http://www.pymol.org.

BI060852X